

Multi-objective Optimal Sizing and Real-time Control of Hybrid Energy Storage Systems for Electric Vehicles

Huilong Yu and Dongpu Cao

Abstract—Hybrid energy storage system (HESS) has been recognized as one of the most promising solutions to overcome the drawbacks of the expensive and short life lithium-ion battery with low power density, by introducing a proper number of supercapacitors. However, the hybridization introduces complicated sizing and energy management problems. This paper aims to investigate the sizing and real-time energy management of a devised HESS for electric vehicles with an electric race car as a case study. In particular, a proposed multi-objective Bi-level optimal sizing and control framework is implemented to find the optimal parameters of the energy management algorithm, the optimal number of the lithium-ion battery cells and the supercapacitor banks. The simulation results have validated the effectiveness of the investigated methodology in minimizing the total mass of the HESS and maximizing the cycle life of the lithium-ion battery.

I. INTRODUCTION

Electric vehicles (EVs) have gained tremendous amount of attentions worldwide to face against the deteriorated headaches related with fossil energy crisis and environment protection problems. Although EVs have already achieved a significant market share after decades of development, they still face upset problems caused by the fast degradation of the high cost lithium-ion batteries. The hybrid energy storage system (HESS) composed by lithium-ion batteries and supercapacitors (SCs) has been recognized as an extremely prospective solution to reduce the size and cost with respect to the conventional energy storage systems (ESSs) [1]–[4]. Nevertheless, the practical performances of a HESS are significantly influenced by the complex sizing and the energy management strategy.

The sizing problem of HESS aims to find the appropriate number of supercapacitor banks and battery cells that minimizing the cost, mass and efficiency of the HESS or to maximize the battery cycle life. In [5], a multi-objective optimization problem was formulated to minimize the overall HESS size and to maximize the battery cycle life, the formulated problem was solved with the sample-based global search oriented Dividing RECTangles (DIRECT) algorithm. Ref. [6] proposed a multi-objective sizing approach based on non-dominated sorting genetic algorithm II (NSGA-II) for a semi-active HESS and obtained the Pareto frontier with

the battery capacity loss and total cost of supercapacitors as objectives. Convex optimization was introduced to solve the formulated sizing and energy management problems of different kinds of HESSs with weighted cost as objective [2], [7].

For the energy management system (EMS) of HESS, both rule based and optimization based approaches are widely researched [8]. Rule based EMS is generally devised according to the engineering experience, heuristics, intuition or mathematical models. There are mainly two kinds of rule based EMS so far. One is the deterministic or heuristic rule-based [9]–[11], which has high stability and real-time performance. The other is conventional Fuzzy Logic Control (FLC) based [12]–[14], which has the features of independence of full mathematical system model and intelligence realizable in real system. Its performance is, nevertheless, determined by fuzzy rules, number and shape of the membership functions (MFs). Optimization approach can be classified into global optimization and real time optimization. Neural network [15], [16], Dynamic Programming (DP) [17], [18], convex programming [7] and other multi-objective optimization [5], [19] based EMSs presented in the literature belong to global optimization. The proposed real time optimization methods to design EMS for HESS consists of model predictive control [17], [20], decoupling method [21], [22], etc.

Most of the aforementioned literature investigated the sizing and energy management problems separately which can not obtain the global optimal performance since the design and control problems of a HESS are actually coupled in practice [23]. We can only obtain the sub-optimal solution when we try to optimize one and fix the other. In order to force against these drawbacks, this work will explore the sizing and real-time energy management problem of the HESS as a coupled problem. With the proposed Bi-level optimal sizing and control framework, we can obtain the Pareto optimal solutions of the formulated problem and achieve both the optimal sizing parameters and the static parameters of the EMS simultaneously for each Pareto optimal solution which are ready for further real-time implementation.

The rest of this work is organized as follows: Section 2 details architecture of the HESS, the Bi-level design and energy management framework and the calculation of the demand power. Section 3 elaborates the modelling of the battery and supercapacitor. Section 4 details the devised FLC based EMS. In section 5, the formulation of the multi-objective optimization problem of the HESS is illustrated. Section 6 and Section 7 illustrate the achieved results and the concluding remarks respectively.

This work was supported by Vehicle Intelligence Pioneers Ltd, Qingdao, China. (Corresponding author: Dongpu Cao)

Huilong Yu is with Vehicle Intelligence Pioneers Inc., Qingdao, China, he is also with the Mechanical and Mechatronics Engineering Department, University of Waterloo, N2L 3G1, Waterloo, Canada. huilong.yu@ieee.org.

Dongpu Cao is with the Mechanical and Mechatronics Engineering Department, University of Waterloo, N2L 3G1, Waterloo, Canada dongpu.cao@uwaterloo.ca.

II. SYSTEM OVERVIEW

A. Details of the electric race car with HESS

The configuration of the devised HESS for the electric race car is demonstrated as Figure 1. The supercapacitor (SC) can output and absorb high peak power by controlling a bidirectional DC/DC converter that interfaces the supercapacitor to the DC link of the battery in parallel. Moreover, the voltage of supercapacitor can be used in a wide range with the help of the DC/DC converter [24]. There is a DC/AC inverter between the DC link and the AC motor that converts direct current to alternating current and power an employed AC motor.

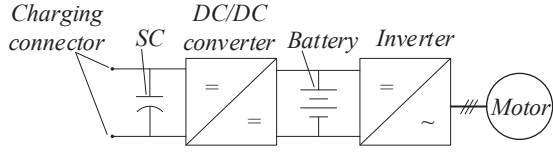


Fig. 1. Configuration of the HESS

The symbols and values of the electric race car parameters are illustrated in Table I.

TABLE I

SYMBOLS AND VALUES OF THE ELECTRIC RACE CAR PARAMETERS

Parameters	Symbol	Value
Vehicle mass (kg)	m_v	570
Aerodynamics coefficient (h^2N/km^2)	$\rho C_d A$	0.075
Rolling resistance coefficient	f	0.016
Mass of the battery cell (kg)	m_{cell}	1.15
Peak power of the battery cell (kW)	P_{cell}	2.6
Voltage constant of the battery cell (V)	E_0	3.43
Total capacity of the battery cell(Ah)	Q_{max}	55
Rated discharge energy of the battery cell(kWh)	E_{cell}	0.196
Polarization resistance of the battery cell (Ω)	K	8.85×10^{-5}
Internal resistance of the battery cell (Ω)	R	1.33×10^{-3}
Voltage amplitude of the battery cell (V)	A	0.761
Time constant inverse of the battery cell (Ah^{-1})	B	0.040
Mass of the supercapacitor bank (kg)	m_{bank}	0.52
Supercapacitor bank capacity(F)	C_{bank}	3400
Rated power of the supercapacitor (kW)	P_{bank}	8
Supercapacitor equivalent series resistance (Ω)	R_s	2.2×10^{-4}
Rated discharge energy of the supercapacitor bank(kWh)	E_{bank}	3.95×10^{-3}
Minimum power requirement on the HESS (kW)	P_{min}	165
Minimum energy requirement on the HESS (kWh)	E_{min}	40
Maximum energy requirement on the HESS (kWh)	E_{max}	42
Maximum total mass of the HESS (kg)	m_{HESS}	280
DC/DC converter efficiency	η_{dc}	0.95
DC/AC converter efficiency	η_{AD}	0.96

B. Bi-level design and control framework

The employed Bi-level optimal design and control framework is presented as Figure 2 [25]. The power demand of the driving profile P_{dem} , the battery state of charge x_{SOC} and supercapacitor state of energy x_{SOE} are the inputs of the FLC based EMS, while the outputs are requested power from the battery P_{reqbat} and from the supercapacitor P_{reqsc} . The outputs of the EMS are the inputs of the battery and supercapacitor modeled in Section III, and the multi-objective optimization algorithm will evaluate the objective functions with the outputs of the HESS model when both

the battery and supercapacitor are exhausted after a number of laps.

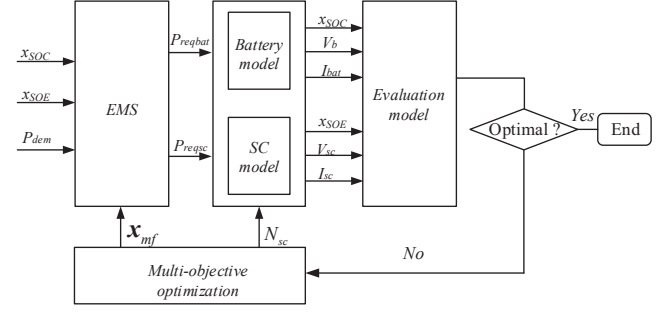


Fig. 2. Framework of the Bi-Level design and control

C. Power demand

The real driving cycle of a race car in Nurburgring circuit is implemented as the test scenario of the HESS sizing and control. The demand acceleration/braking power is calculated by Equation (1). The corresponding velocity profile v , acceleration profile a and demand power P_{dem} are demonstrated in Figure 3.

$$P_{dem} = \left(\frac{1}{2} \rho C_d A v^2 + f m_v g + m_v a \right) v \quad (1)$$

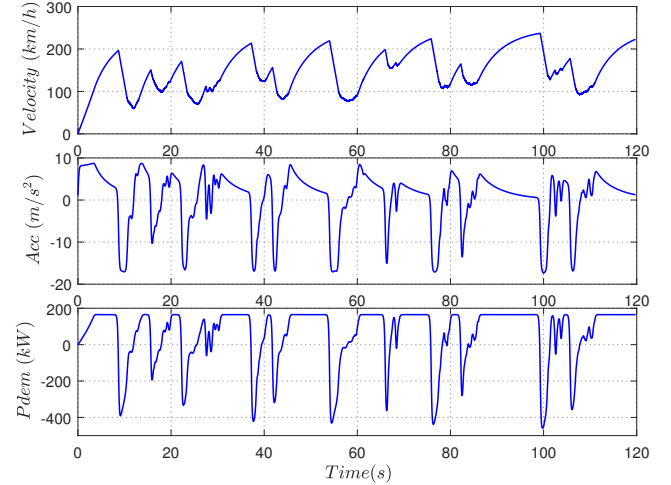


Fig. 3. Power demand in Nurburgring circuit

III. MODELLING OF THE HESS

A. Battery model

In this work, a modified Shepherd model is employed to represent the dynamics of the battery during charging and discharging process [26]. The dynamic battery model are presented as Equation (2) and Equation (3) with the assumption that the internal resistance is constant and the thermal behavior of the battery is neglected.

Discharge:

$$V_{batt} = E_0 - K \frac{Q_{max}}{Q_{max} - it} - K \frac{Q_{max}}{Q_{max} - it} i - Ri + Ae^{(-B \cdot it)} \quad (2)$$

Charge:

$$V_{batt} = E_0 - K \frac{Q_{\max}}{Q_{\max} - it} - K \frac{Q_{\max}}{it - 0.1Q_{\max}} i - Ri + Ae^{(-B \cdot it)} \quad (3)$$

where V_{batt} is the battery voltage (V), E_0 is the voltage constant (V), K is the polarization constant, Q_{\max} is the total capacity, i is the battery current, R is the internal resistance, The A (V) is the voltage amplitude, B (Ah^{-1}) is the time constant inverse of the exponential zone. The battery discharge ($i > 0$) or charge ($i < 0$) it is denoted as

$$it = \int idt. \quad (4)$$

B. Battery cycle life model

A revised semi-empirical model based on Arrhenius equation which is widely studied and validated with large scale experiments is employed in this work [27]. As presented in Equation (5) to Equation (8), the capacity loss of this model is expressed as a function of the discharge current rate C_{rate} , temperature T and ampere-hour throughout A_h ,

$$Q_{loss} = A_p \exp\left(\frac{-E_a}{R_g T}\right) (A_h)^z \quad (5)$$

where Q_{loss} is the battery capacity loss, A_p is the pre-exponential factor, E_a is the activation energy from Arrhenius law (J), R_g is the gas constant of 8.314, T is the absolute temperature (K), A_h is the Ah-throughput, which represents the amount of charge delivered by the battery during cycling.

The pre-exponential factor A_p in Equation (5) is proved to be sensitive to the discharge current rate C_{rate} with experiments in [28], and it can be denoted with a fitting Equation (6) [29],

$$\ln A_p = a \cdot \exp(-b \cdot C_{rate}) + c. \quad (6)$$

The activation energy E_a can be fitted as a linear function of discharge current rate [28],

$$E_a = d + e \cdot C_{rate} \quad (7)$$

where $a = 1.345$, $b = 0.2563$, $c = 9.179$, $d = 46868$, $e = -470.3$ are the fitting parameters of the battery cycle life model.

The Ah-throughput can be expressed as

$$A_h = N_{cycle} \int_0^{t_f} \frac{i}{3600} dt \quad (8)$$

where N_{cycle} is the number of using cycles, i is the discharge current, t_f is the end time of the current profile.

C. Supercapacitor Model

A simplified supercapacitor model in [30] is adopted in this work. The efficiency of the DC/DC converter η_{dc}

between the supercapacitor and the DC link is assumed to be a constant value of 0.95. The related equations are:

$$\dot{V}_{ct} = \begin{cases} -\frac{V_{ct} - \sqrt{V_{ct}^2 - 4R_{sct}P_{reqsc}/(\eta_{AD}\eta_{dc})}}{2C_{sct}R_{sct}} & P_{reqsc} \geq 0 \\ -\frac{V_{ct} - \sqrt{V_{ct}^2 - 4R_{sct}P_{reqsc}\eta_{AD}\eta_{dc}}}{2C_{sct}R_{sct}} & P_{reqsc} < 0 \end{cases} \quad (9)$$

$$x_{SOE} = \frac{V_{ct}^2}{V_{ctmax}^2} \quad (10)$$

where $V_{ct} = V_c N_{sc}$ is the total open circuit voltage of the supercapacitor pack assuming that all banks have a uniform behavior, $R_{st} = N_{sc} R_s$ is the total equivalent series resistance, P_{reqsc} is the demand power from the supercapacitor, η_{dc} is the efficiency of the DC/DC converter, $C_{sct} = C_{bank}/N_{sc}$ is the total capacity, SOE is the state of energy, V_{ctmax} is the initial open circuit voltage, V_c is the open circuit voltage of one supercapacitor, N_{sc} is the total number of the banks, R_s is the series resistance of one supercapacitor.

The actual total output power of the supercapacitor is represented as

$$P_{sc} = V_{ct} \cdot \frac{V_{ct} - \sqrt{V_{ct}^2 - 4R_{st}P_{reqsc}/\eta_{AD}\eta_{dc}}}{2R_{st}}. \quad (11)$$

IV. EMS BASED ON VECTORIZED FUZZY CONTROLLER

The devised EMS in this work is based on fuzzy logic control (FLC), which has the features of real-time, adaptive and intelligent [31], [32]. It allows different operators to merge the nonlinearities and uncertainties in the best way and incorporate heuristic control in the form of if-then rules. A typical FLC is composed of the if-then fuzzy rules, fuzzification, fuzzy inference engine and defuzzification modules. Generally, the user just needs to devise his own fuzzy rules and membership functions.

A. Fuzzy rules

For the FLC based EMS, the designed fuzzy rules established the mapping relationships between the inputs: P_{dem} , x_{SOC} , x_{SOE} and the output P_{reqsc} . The devised fuzzy rules in this work is demonstrated as Figure 4.

B. Membership functions

As demonstrated in Figure 5, there are 28 parameters of the devised membership functions plus one design parameter of the HESS in one page of parameters to be optimized. The design vector \mathbf{p} is constrained by defining \mathbf{p}_{min} and \mathbf{p}_{max} .

In order to improve the optimization efficiency, a developed vectorized fuzzy inference system (VFIS) in [25] is implemented in this work. The dimension of the to be optimized membership function vector is $\mathcal{R}^{28 \times N_p}$, where N_p is the number of pages of the VFIS.

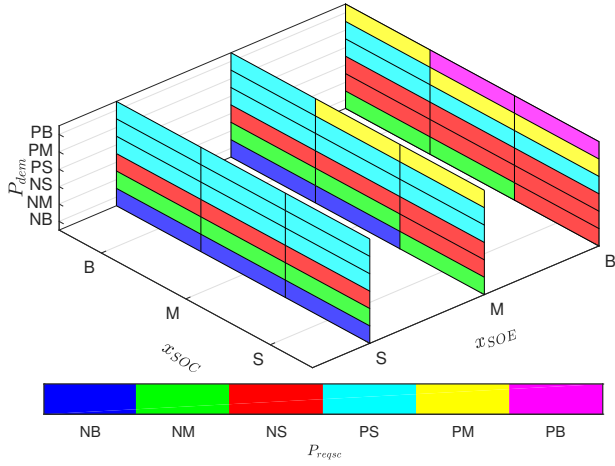


Fig. 4. Fuzzy rules for the EMS of the HESS

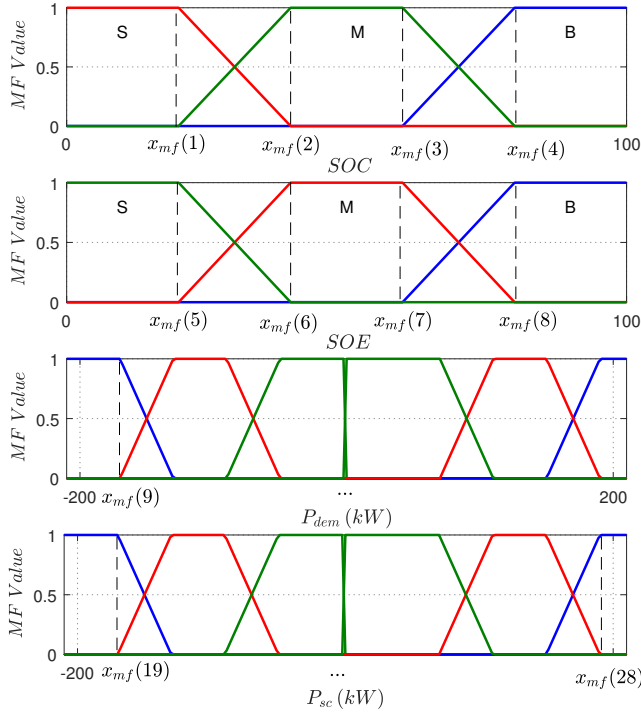


Fig. 5. The design parameters of the MFs for the EMS

V. PROBLEM SIMULATION

A. Problem formulation

The objective of this work is to find the optimal sizing parameter N_{bat} , N_{sc} and the parameter vector \mathbf{x}_{mf} defining the membership functions which are respectively the key parameters of HESS design and the real-time FLC based EMS. The optimized $[N_{bat}, N_{sc}]$ will help to minimize the total mass of the HESS J_{mass} and The optimized EMS with \mathbf{x}_{mf} will output the requested control command series $\mathbf{u}(t) = [P_{reqbat}, P_{reqsc}]$ that can maximize the battery cycle life $J_{lifebat}$ on a given race circuit:

$$\max J = [-J_{mass}(\mathbf{p}), J_{lifebat}(\mathbf{x}(t), \mathbf{u}(t), \mathbf{p})] \quad (12)$$

subject to:

$$\begin{aligned} N_{bat}P_{cell} + N_{sc}P_{bank} &> P_{min} \\ E_{min} < N_{bat}E_{cell} + N_{sc}E_{bank} < E_{max} \\ N_{bat}m_{cell} + N_{sc}m_{bank} &< m_{HESS} \\ x_{mf}(i) < x_{mf}(i+1) \end{aligned} \quad (13)$$

where the first constraint makes sure that the total power can meet the power demand of the race car, the second one ensures the available driving range by setting a minimum energy capacity value while the up boundary is to limit the maximum storage of the HESS and avoid unnecessary search. The third one is to constraint the maximum mass of the HESS, while the last one is to guarantee the right relationship of the neighbored parameters of the membership functions. In addition to the constraints during the optimization, the usage and terminal conditions of the HESS are also devised with additional constraints on the currents, voltage and state of the charge of the battery and supercapacitor respectively.

The total mass of the HESS is denoted as

$$J_{mass} = N_{bat}m_{cell} + N_{sc}m_{bank}. \quad (14)$$

The available cycle life of the lithium-ion battery is deduced as Equation (15) with a given capacity loss limit $Q_{losslim} = 20\%$ based on equations (6) to (8),

$$J_{lifebat} = \left[\frac{Q_{losslim}}{A_p \exp\left(\frac{-E_a}{R_s T}\right)} \right]^{1/z} / \left(\int_0^{t_f} \frac{i}{3600} dt \right). \quad (15)$$

VI. RESULTS

The formulated problem is solved with a controlled elitist NSGA which is a variant of NSGA-II [33], the population size is set to 2000 and the iteration is terminated after 278 generations. More than 550000 solutions have been evaluated and each solution is associated with the optimized design parameters of both the HESS and the FLC based EMS.

As it can be observed from Figure 6, the HESS can have small size but short battery life when there are very few supercapacitors integrated. This situation can be improved to a quite appropriate level with about 30 supercapacitor banks and an optimized EMS. Figure 6 also demonstrates that the initial solution utilizing 50 supercapacitors and 200 battery cells with the original EMS can obtain a HESS with $J_{mass} = 256$ kg and $J_{lifebat} = 2951$. While a chosen solution on the Pareto frontier when $N_{sc} = 32, N_{bat} = 203$ with the optimized EMS can achieve an enhanced HESS with $J_{mass} = 249$ kg and $J_{lifebat} = 3081$.

The integrated design parameters of the membership functions after optimization is compared with the initial devised in Figure 7. The optimized membership functions in solid lines are quite different with the original membership functions in dotted lines and we can image that it is unlikely to devise such membership functions manually.

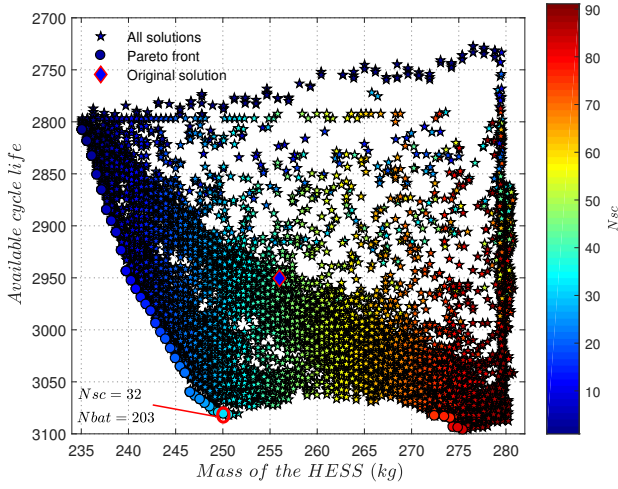


Fig. 6. Multi-objective optimal sizing and control solutions

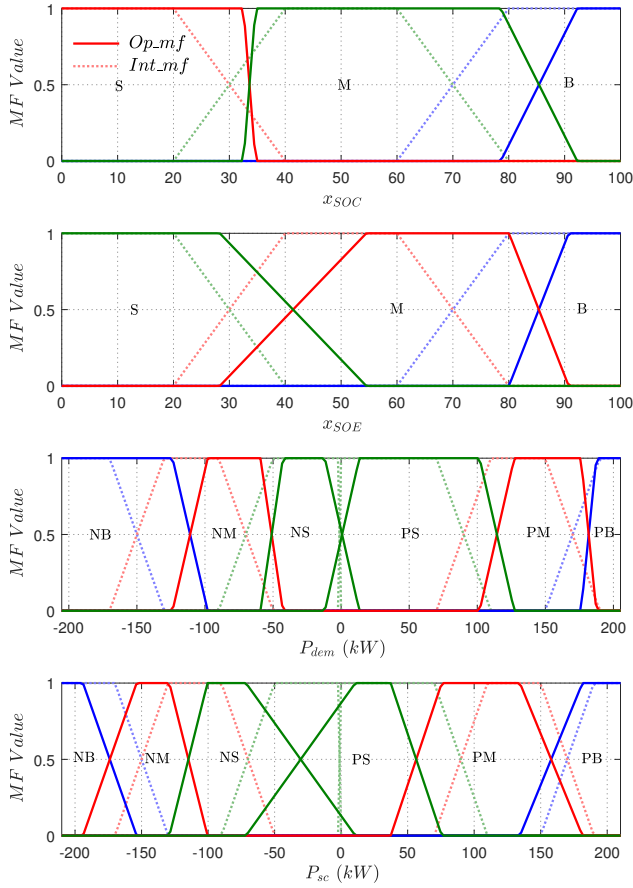


Fig. 7. The initial and optimized membership functions when $N_{sc} = 32$, $N_{bat} = 203$

Figure 8 (a) demonstrates that the power requested from the battery is reduced in the whole profile after optimization. It is shown in Figure 8 (b) that the regenerated power by the supercapacitors during the braking operations is increased and the output power of the supercapacitors can assist for a longer time compared with the initial solution. As it is

illustrated in Figure 8 (c), the original EMS tends to fully discharge the supercapacitors in a very short time after starting the operation and it is mostly under the exhausted condition during the driving profile, while the optimized solution is able to maintain the SOE at a higher level with more regenerative braking power. The optimized HESS and EMS can take fully advantage of the implemented supercapacitors, which can recover more energy in order to output power for a longer time and reduce the average power demand from the battery. The Bi-level optimal design and control framework will be more effective in conventional electric vehicles with HESS since most of them do not operate in such extreme conditions.

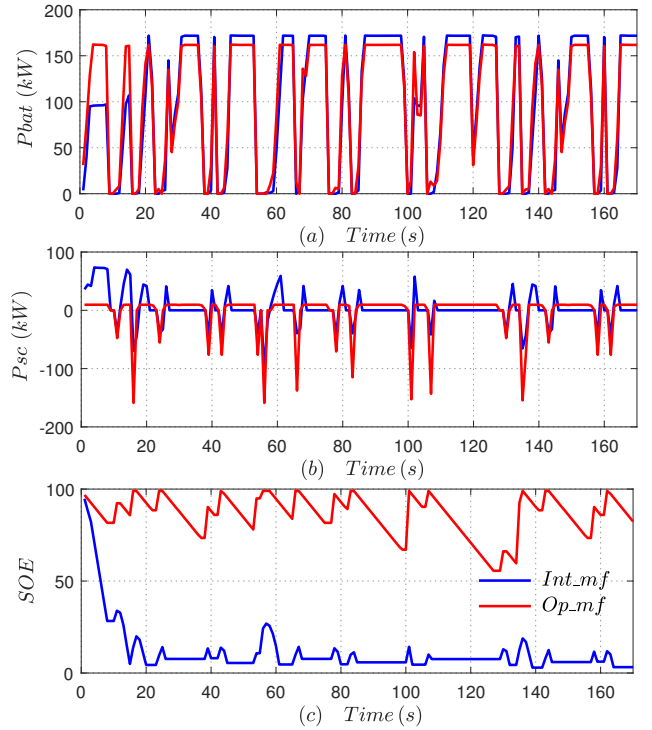


Fig. 8. Detail comparison of the initial and optimized solutions

VII. CONCLUSIONS

Utilizing a large number of supercapacitors in a HESS will increase the total mass significantly with only limited improvement of the battery cycle life, this is due to the fact that the energy density of the supercapacitor is very poor and it can be exhausted very fast even it has high power density. The optimal solution is to implement a proper number of superconductors and recover the braking energy with them as much as possible during the whole profile and then output it to reduce the battery discharging power. The implemented multi-objective Bi-level optimal design and control framework is able to obtain the Pareto optimal frontier with the total mass and battery cycle life as objective functions. A preferred trade-off solution with sized HESS and optimized real-time FLC based EMS can be chosen from the Pareto optimal frontier. The simulation results

has proved that multi-objective Bi-level optimal design and control framework can improve both concerned objectives effectively and this methodology also can be applied in the optimization of general kinds of design and real-time control problems.

REFERENCES

- [1] H. Yu, D. Tarsitano, X. Hu, and F. Cheli, "Real time energy management strategy for a fast charging electric urban bus powered by hybrid energy storage system," *Energy*, vol. 112, pp. 322–331, 2016.
- [2] X. Hu, L. Johannesson, N. Murgovski, and B. Egardt, "Longevity-conscious dimensioning and power management of the hybrid energy storage system in a fuel cell hybrid electric bus," *Applied Energy*, vol. 137, pp. 913–924, 2015.
- [3] T. Ma, H. Yang, and L. Lu, "Development of hybrid battery supercapacitor energy storage for remote area renewable energy systems," *Applied Energy*, vol. 153, pp. 56–62, 2015.
- [4] O. Ahmed and J. Bleijs, "An overview of dc/dc converter topologies for fuel cell-ultracapacitor hybrid distribution system," *Renewable and Sustainable Energy Reviews*, vol. 42, no. Supplement C, pp. 609 – 626, 2015.
- [5] J. Shen, S. Dusmez, and A. Khaligh, "Optimization of sizing and battery cycle life in battery/ultracapacitor hybrid energy storage systems for electric vehicle applications," *IEEE Transactions on Industrial Informatics*, vol. 10, no. 4, pp. 2112–2121, 2014.
- [6] Z. Song, J. Li, X. Han, L. Xu, L. Lu, M. Ouyang, and H. Hofmann, "Multi-objective optimization of a semi-active battery/supercapacitor energy storage system for electric vehicles," *Applied Energy*, vol. 135, no. 0, pp. 212–224, 2014.
- [7] X. Hu, N. Murgovski, L. M. Johannesson, and B. Egardt, "Comparison of three electrochemical energy buffers applied to a hybrid bus powertrain with simultaneous optimal sizing and energy management," *IEEE Transactions on Intelligent Transportation Systems*, vol. 15, no. 3, pp. 1193–1205, 2014.
- [8] S. F. Tie and C. W. Tan, "A review of energy sources and energy management system in electric vehicles," *Renewable and Sustainable Energy Reviews*, vol. 20, pp. 82 – 102, 2013.
- [9] Y.-H. Hung and C.-H. Wu, "An integrated optimization approach for a hybrid energy system in electric vehicles," *Applied Energy*, vol. 98, pp. 479–490, 2012.
- [10] S. Lu, K. a. Corzine, and M. Ferdowsi, "A new battery/ultracapacitor energy storage system design and its motor drive integration for hybrid electric vehicles," *IEEE Transactions on Vehicular Technology*, vol. 56, no. 4 I, pp. 1516–1523, 2007.
- [11] C. Xiang, Y. Wang, S. Hu, and W. Wang, "A New Topology and Control Strategy for a Hybrid Battery-Ultracapacitor Energy Storage System," *Energies*, vol. 7, no. 5, pp. 2874–2896, 2014.
- [12] M. Zandi, A. Payman, J. P. Martin, S. Pierfederici, B. Davat, and F. Meibody-Tabar, "Energy management of a fuel cell/supercapacitor/battery power source for electric vehicular applications," *IEEE Transactions on Vehicular Technology*, vol. 60, no. 2, pp. 433–443, 2011.
- [13] C. Xie, X. Xu, P. Bujlo, D. Shen, H. Zhao, and S. Quan, "Fuel cell and lithium iron phosphate battery hybrid powertrain with an ultracapacitor bank using direct parallel structure," *Journal of Power Sources*, vol. 279, pp. 487–494, 2015.
- [14] S. Dusmez and A. Khaligh, "A Supervisory Power-Splitting Approach for a New Ultracapacitor/Battery Vehicle Deploying Two Propulsion Machines," *IEEE Transactions on Industrial Informatics*, vol. 10, no. 3, pp. 1960–1971, 2014.
- [15] Y. Ates, O. Erdinc, M. Uzunoglu, and B. Vural, "Energy management of an FC/UC hybrid vehicular power system using a combined neural network-wavelet transform based strategy," *International Journal of Hydrogen Energy*, vol. 35, no. 2, pp. 774–783, 2010.
- [16] J. Moreno, M. E. Ortúzar, J. J. W. Dixon, M. Ortúzar, J. J. W. Dixon, "Energy-management system for a hybrid electric vehicle, using ultracapacitors and neural networks," *IEEE Transactions on Industrial Electronics*, vol. 53, no. 2, pp. 614–623, 2006.
- [17] D. Rotenberg, A. Vahidi, and I. Kolmanovsky, "Ultracapacitor assisted powertrains: Modeling, control, sizing, and the impact on fuel economy," *IEEE Transactions on Control Systems Technology*, vol. 19, no. 3, pp. 576–589, 2011.
- [18] Z. Song, H. Hofmann, J. Li, X. Han, and M. Ouyang, "Optimization for a hybrid energy storage system in electric vehicles using dynamic programming approach," *Applied Energy*, vol. 139, no. Dc, pp. 151–162, 2015.
- [19] H. Yin, C. Zhao, M. Li, and C. Ma, "Utility Function-Based Real-Time Control of A Battery Ultracapacitor Hybrid Energy System," *IEEE Transactions on Industrial Informatics*, vol. 11, no. 1, pp. 220–231, 2015.
- [20] B. Hredzak, V. G. Agelidis, and M. Jang, "A model predictive control system for a hybrid battery-ultracapacitor power source," *IEEE Transactions on Power Electronics*, vol. 29, no. 3, pp. 1469–1479, 2014.
- [21] J. M. Blanes, R. Gutiérrez, A. Garrigós, J. L. Lizán, and J. M. Cuadrado, "Electric vehicle battery life extension using ultracapacitors and an FPGA controlled interleaved buck-boost converter," *IEEE Transactions on Power Electronics*, vol. 28, no. 12, pp. 5940–5948, 2013.
- [22] M. Uzunoglu and M. S. Alam, "Modeling and analysis of an FC/UC hybrid vehicular power system using a novel-wavelet-based load sharing algorithm," *IEEE Transactions on Energy Conversion*, vol. 23, no. 1, pp. 263–272, 2008.
- [23] H. Yu, F. Castelli-Dezza, and F. Cheli, "Optimal powertrain design and control of a 2-iwd electric race car," in *2017 International Conference of Electrical and Electronic Technologies for Automotive*, June 2017, pp. 1–7.
- [24] J. Cao and A. Emadi, "A new battery/ultracapacitor hybrid energy storage system for electric, hybrid, and plug-in hybrid electric vehicles," *IEEE Transactions on power electronics*, vol. 27, no. 1, pp. 122–132, 2012.
- [25] H. Yu, F. Cheli, F. Castelli-Dezza, D. Cao, and F.-Y. Wang, "Multi-objective Optimal Sizing and Energy Management of Hybrid Energy Storage System for Electric Vehicles," *ArXiv e-prints*, Jan. 2018.
- [26] O. Tremblay, "Experimental validation of a battery dynamic model for ev applications experimental validation of a battery dynamic model for ev applications," in *24th International Battery, Hybrid and Fuel Cell Electric Vehicle Symposium and Exhibition 2009, EVS 24*, vol. 2, 2009, pp. 930–939.
- [27] J. Wang, P. Liu, J. Hicks-Garner, E. Sherman, S. Soukiazian, M. Verbrugge, H. Tataria, J. Musser, and P. Finamore, "Cycle-life model for graphite-LiFePO₄ cells," *Journal of Power Sources*, vol. 196, no. 8, pp. 3942–3948, 2011.
- [28] R. Wang, Y. Chen, D. Feng, X. Huang, and J. Wang, "Development and performance characterization of an electric ground vehicle with independently actuated in-wheel motors," *Journal of Power Sources*, vol. 196, no. 8, pp. 3962–3971, 2011.
- [29] J. Shen, A. Hasanzadeh, and A. Khaligh, "Optimal power split and sizing of hybrid energy storage system for electric vehicles," in *2014 IEEE Transportation Electrification Conference and Expo (ITEC)*, 2014, pp. 1–6.
- [30] L. Zhang, X. Hu, Z. Wang, F. Sun, and D. G. Dorrell, "A review of supercapacitor modeling, estimation, and applications: A control/management perspective," *Renewable and Sustainable Energy Reviews*, vol. 81, pp. 1868 – 1878, 2018.
- [31] H. Wang, F.Y. and Kim, "Implementing adaptive fuzzy logic controllers with neural networks," *Analytical Chemistry*, vol. 3, no. 2, pp. 165–180, 1995.
- [32] Xiaobo Shi, P. Lever, and Fei-Yue Wang, "Experimental robotic excavation with fuzzy logic and neural networks," in *Proceedings of IEEE International Conference on Robotics and Automation*, vol. 1. IEEE, pp. 957–962.
- [33] K. Deb, "Multi-objective optimization using evolutionary algorithms: an introduction," *Multi-objective evolutionary optimisation for product design and manufacturing*, pp. 1–24, 2011.